Isospin splitting of giant resonances in ^{13}C and ^{17}O

D. J. Albert,* Anton Nagl, Jacob George, and R. F. Wagner†
The Catholic University of America, Washington, D. C. 20064 ‡

H. Überall
The Catholic University of America, Washington, D. C. 20064 ‡
and Naval Research Laboratory, Washington, D. C. 20375
(Received 31 January 1977)

The two-particle, one-hole shell model with a harmonic oscillator basis is employed for a calculation of isospin-split giant resonance states in ^{13}C and ^{17}O that can be reached from the ground state by $\Delta T = 0,1$ transitions of type $E1$ or $M2$. Residual forces used were a zero-range Soper mixture as well as the separable Tabakin potential. We calculate photoabsorption strengths which for ^{13}C agree with the available data and with a previous calculation of Easlea using the Soper force; for the Tabakin force, this agreement is achieved without Easlea's *ad hoc* modification of the interaction. We also evaluate the inelastic form factors for electroexcitation of the ^{13}C resonance levels, thereby identifying isospin and spin-isospin collective states.

[NUCLEAR REACTIONS ^{13}C calculated photonuclear cross sections, electron scattering form factors of giant and pygmy resonances $(T_>, T_<)$; ^{17}O calculated photonuclear cross sections. Used two-particle, one-hole shell model.]

I. INTRODUCTION

In photonuclear studies of the giant resonance region of light nuclei,[1,2] much attention has been paid to the self-conjugate nuclei (with ground state isospin $T_0 = 0$), especially those with closed (sub) shells such as ^{12}C, ^{16}O, ^{28}Si, and ^{40}Ca. The non-self-conjugate nuclei ($T_0 \neq 0$), including those of closed shell ± 1 extra particle character, have been studied to a lesser degree. Recent experiments have produced some data on the $T_0 \neq 0$ nuclei. There now exist several measurements of (γ, n) reactions[3-8] and (γ, p) reactions[6,7] on ^{13}C and ^{13}N targets and of (p, γ) reactions[9-11] on ^{12}C. To our knowledge, only one report[12] on $^{16}O(p, \gamma)$ is available.

The $T_0 \neq 0$ nuclei should present an interesting feature worth investigating, namely, an "isospin splitting" of their giant resonance peak into two components as predicted by Fallieros, Goulard and co-workers[13] in general and by Easlea[14] for ^{13}C in particular. Due to the predominant isovector nature of the $E1$ photoexcitation operator,[15] the giant dipole resonances seen in the self-conjugate nuclei are $T = 1$ states, while in $T_0 \neq 0$ nuclei they consist of separate $T_> = T_0 + 1$ and $T_< = T_0$ levels expected[13] to be split by several MeV (with $T_>$ lying higher). For small values of T_0, most of the dipole strength should still be concentrated in the $T_>$ resonance; but for increasing T_0, most of the strength would shift[13] into the $T_<$ state, so that e.g., for $^{90}Zr(T_0 = 5)$, the $T_>$ state is so small that it could be found only after a careful search.[16] For the lighter nuclei, the isospin splitting was confirmed[14,17,18] in ^{13}C and[19] in ^{26}Mg.

We have applied[20] the particle-hole shell model in the Tamm-Dancoff approximation[21] to the nuclei ^{13}C and ^{17}O with one valence nucleon outside the (assumed) closed cores of ^{12}C and ^{16}O, respectively, with the purpose of obtaining the isospin splitting of the photonuclear giant dipole ($E1$) resonance for these particular cases.[22,23] Furthermore, the electron scattering form factors[24] $\mathfrak{M}_1(q)$, $\mathcal{T}_1^E(q)$, and $\mathcal{T}_2^M(q)$ were calculated as functions of momentum transfer q for the giant resonance states in ^{13}C reached by $\Delta T = 0$ and 1 transitions of type $C1$, $E1$, and $M2$, in order to determine the isospin or spin-isospin character[24-26] of these levels; the results are compared with the electroexcitation data of Bergstrom *et al.*[27] The calculation was carried out using two different types of residual forces: (a) a simple δ-function potential with a Soper exchange mixture[14] and (b) the "realistic" Tabakin potential[28] which is smooth and separable. Spurious ($T = \frac{1}{2}$) states were removed by the Baranger-Lee method.[29] The calculated photoabsorption strength for ^{13}C agrees with the available data and with the calculation of Easlea[14,17] who employed the Soper force; for the Tabakin force, this agreement is achieved without using Easlea's *ad hoc* modification of the Soper interaction needed to reproduce the 4.43 MeV level in ^{12}C. For ^{17}O, we have compared our prediction of the photoabsorption strength with experimental results obtained by Harakeh, Paul, and Gorodetzky[12]; our calculation here shows no strict separation of the $T = \frac{1}{2}$ and $T = \frac{3}{2}$ resonances. The theoretical photoabsorption strengths are also

TABLE I. Single-particle energies for ^{13}C and ^{17}O (in MeV).

	$(1s_{1/2})^{-1}$	$(1p_{3/2})^{-1}$	$(1p_{1/2})$	$(2s_{1/2})$	$(1d_{5/2})$	$(1d_{3/2})$	$(1f_{7/2})$	$(2p_{3/2})$	$(1f_{5/2})$	$(2p_{1/2})$
^{13}C	35	18.7	−4.9	−1.9	−1.1	3.4				
^{17}O	45	21.7	−15.6	−3.3	−4.1	0.9	18	23	25	26

shown to agree with an isospin sum rule of O'Connell.[30]

II. CALCULATION FOR ^{13}C

The method of calculation of nuclear levels and wave functions in the framework of the particle-hole model is standard[14,21] and will here not be dealt with in detail. A pure shell model state (of a filled $1p_{3/2}$ subshell, with one valence neutron in the $1p_{1/2}$ shell) is assumed for the ^{13}C ground state; the two-particle, one-hole excited basis states are formed out of this by core excitation, i.e., by promoting either a $1p_{3/2}$ shell particle to the $2s$-$1d$ shell states or by promoting a $1s_{1/2}$ particle into the empty $1p_{1/2}$ levels; in addition, promotion of the valence particle gives one-particle excited states. The positions of the single-particle levels are given in Table I; they are taken from Vinh-Mau and Brown's article[31] on ^{12}C, where they represent the low-excited states of the nuclei adjacent to ^{12}C. The $(1p_{3/2})^{-1}$ hole energy is assumed to be the ground state energy of ^{11}C. The $(1s_{1/2})^{-1}$ hole is assigned its energy from a $(p, 2p)$ experiment[32] which reveals a very broad level for the binding energy of the $1s$ nucleon. The $1p_{1/2}$ particle level is easily found from the ground state of ^{13}C. The excited $\frac{1}{2}^+$ and $\frac{5}{2}^+$ states of ^{13}C are interpreted as the $2s_{1/2}$ and $1d_{5/2}$ single-particle states. The $1d_{3/2}$ state is taken from data on a (d,p) reaction.[33] Harmonic oscillator wave functions are used, with an oscillator parameter taken from Lewis and Walecka's[34] calculation for ^{12}C, adjusted for the $A^{1/3}$ dependence.

Using this basis, we diagonalize the energy matrix containing the above-mentioned residual interactions, to obtain the intermediate-coupling particle-hole wave functions. The Soper interaction employed here is of the type

$$v(1,2) = V_0\delta(\vec{r}_1 - \vec{r}_2)(0.865 + 0.135\vec{\sigma}_1 \cdot \vec{\sigma}_2) \; ; \qquad (1)$$

its strength and the oscillator parameter used are listed in Table II. The Tabakin potential is taken from Ref. 28 and from Clement and Baranger.[35,36] Our Soper parameters are the same ones which Easlea[14] employed, so that comparison with his results provides a check on our (and Easlea's) calculation.

Easlea noticed that with the use of the Soper potential, an additional strengthening of the interaction in the $j^\pi = 2^+$, $\tau = 0$ configuration of the valence particle and the hole was needed:

$$V_0 \to V_0(1 + 2.68\delta_{0\tau}\delta_{2^+ j^\pi}) \; , \qquad (2)$$

since this configuration represents the $J^\pi = 2^+$, $T = 0$ lowest excited (vibrational) state in ^{12}C which must be found by the calculation to lie at the experimental energy. (The need for the introduction of this *ad hoc* force became urgent by Easlea's observation that without it, the calculated photoabsorption cross section would not reproduce the observed[3] peak at ~12–15 MeV.) We have performed our Soper calculation including Eq. (2), and the Tabakin calculation with and without it.

A. Photoabsorption cross section

We first calculated the electric dipole strengths D^2 of the $T=\frac{1}{2}$ and $T=\frac{3}{2}$ states reached by the $\Delta T = 1$, $\Delta L = 1$ electric transitions[37] (i.e., the $J=\frac{1}{2}$ and $\frac{3}{2}$ states). The corresponding photoabsorption cross section is plotted in Fig. 1 for the Soper interaction and in Fig. 2 for the Tabakin potential, in the form of a histogram with an arbitrary 2 MeV width of each level. A comparison of the several experimental photoabsorption cross sections available in the literature are shown in Fig. 3. The data are from Berman,[5] Cook,[3] Muirhead *et al.*,[4] and from Denisov *et al.*[6] as indicated.

In Figs. 1 and 2, we plot the quantity ωD^2 which is proportional to the integrated cross section, ω being the excitation energy. For comparison, these figures also show selected experimental data as indicated. Figure 1 is very similar to a corresponding figure in Ref. 17 showing Easlea's cross section, with which our calculation agreed to within 1%. The $T=\frac{3}{2}$ identification (cross-hatched) of the 25 MeV peak is confirmed by its absence in Fisher's (p, γ_0) data.[9] The $T=\frac{3}{2}$ states

TABLE II. ^{13}C parameters.

Oscillator parameter b	0.38 fm^{-2}
Soper interaction strength[a]	10.2 MeV fm^6
$j^\pi = 2^+$ interaction strength	2.68 MeV fm^6

[a]Given in terms of $V_0/4\pi b^3$, cf. Eq. (1).

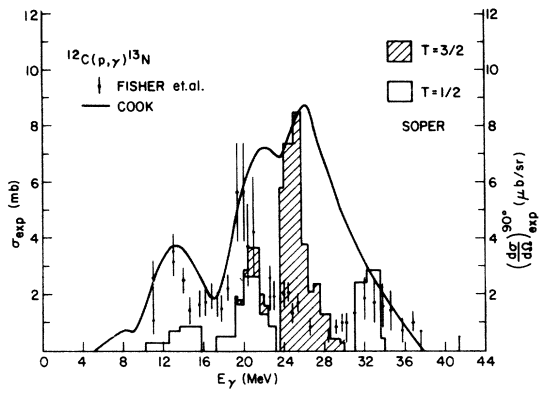

FIG. 1. Electric dipole photoabsorption cross section of ^{13}C calculated with the Soper potential, plotted as a histogram (arbitrary units). $^{12}C(p,\gamma_0)^{13}N$ differential cross sections ($\theta = 90°$) measured by Fisher (Ref. 9) and $^{13}C(\gamma, xn)^{12}C$ total cross sections measured by Cook (Ref. 3) are also shown, with corresponding scales on either side of the figure.

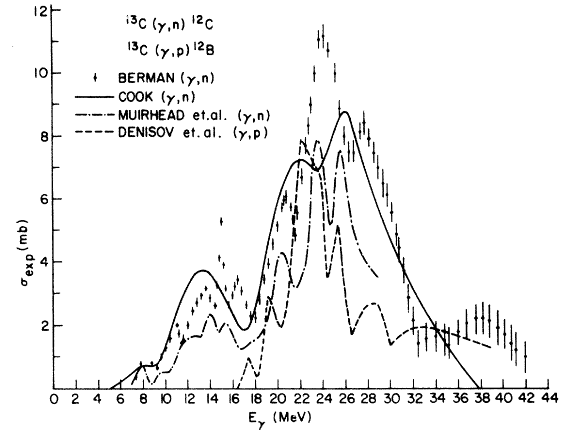

FIG. 3. Experimental photoabsorption cross sections for the reaction $^{13}C(\gamma, xn)^{12}C$ from Cook (Ref. 3), Berman (Ref. 5), and Muirhead *et al.* (Ref. 4) and for the reaction $^{13}C(\gamma, p)^{12}B$ from Denisov *et al.* (Ref. 6).

always have the two particles coupled to intermediate isospin $t = 1$; the main component at 25 MeV is well separated[38] from the $T = \frac{1}{2}$ peak at 20 MeV. The small "pygmy" peak at 15 MeV is due to the mixing of single-particle excitation and core vibration. (The $T = \frac{1}{2}$ states can have a coupling to intermediate $t = 0$ or $t = 1$.) The experiments agree quite well both with the Soper cross section and with the very similar Tabakin results of Fig. 2, which were obtained by us without[39] the use of Eq. (2). The higher peaks above 30 MeV result from $(1s_{1/2})^{-1}$ configurations. There are as yet no experimental results concerning their existence, although similar peaks in the ^{12}C photoabsorption cross section have not been confirmed experimentally.

O'Connell[30] has given an isospin sum rule for bremsstrahlung-weighted cross sections (σ_b), which, for ^{13}C(g.s., $T = \frac{1}{2}$) can be written as

$$\sigma_b(\tfrac{1}{2}) - \tfrac{1}{2}\,\sigma_b(\tfrac{3}{2}) = \frac{\pi^2 e^2}{3\hbar c}\,(N\langle R_n^{\,2}\rangle - Z\langle R_p^{\,2}\rangle)\,. \qquad \text{(3a)}$$

Here,

$$\sigma_b(T) = \int_0^\infty dE\,\frac{\sigma(T)}{E}\,, \qquad \text{(3b)}$$

$\langle R_n^{\,2}\rangle$ and $\langle R_p^{\,2}\rangle$ are the mean square neutron and proton distribution radii, respectively. Assuming that the photoabsorption cross section below 22.5 MeV is primarily due to $T = \frac{1}{2}$ states and above this energy due to $T = \frac{3}{2}$ states, O'Connell gets for the left-hand side of Eq. (3a), using Cook's[3] experimental results, the value 1.15 mb. Setting $R_n = R_p = 2.36$ fm in accordance with electron scattering data,[40] the right-hand side of Eq. (3a) becomes[41] 1.34 mb. Against these results, our model predicts the values of 1.12 mb with the Soper interaction and 0.86 mb with the Tabakin interaction for the left-hand side of Eq. (3a), where we have normalized our quantity $\sigma_b(\frac{1}{2}) + \sigma_b(\frac{3}{2})$ to that from Cook's[3] experimental values. We note parenthetically that since experimental values of R_n and R_p, which are not necessarily the same as the values predicted by our model, were used to calculate the right-hand side of Eq. (3a), the equation need not be regarded as an identity.

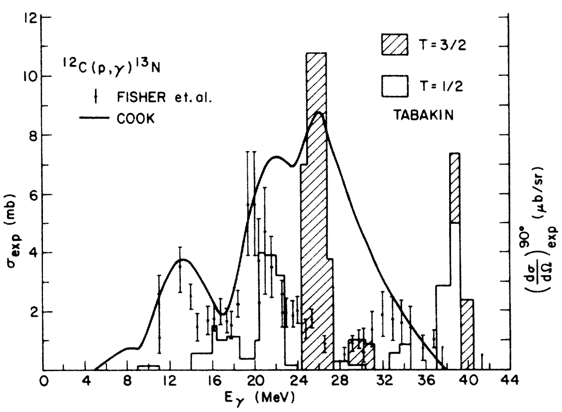

FIG. 2. Same as Fig. 1 except that Soper interaction is replaced by Tabakin interaction.

B. Electron scattering cross section

We have also calculated the electron scattering form factors for ^{13}C with our model. These form factors provide new information on the model for two reasons.[24] First, electron scattering involves the "longitudinal" Coulomb interaction as well as the "transverse" electric and magnetic interactions, while photoabsorption involves only the "transverse" interaction. Secondly, it offers a chance to study the different matrix elements involved as functions of the momentum transferred from the electron to the nucleus. The calculated form factors were compared with experimental ones obtained by Bergstrom *et al.*[27] The results are shown in Fig. 4 (incident electron energy E_i = 55.4 MeV, scattering angle $\theta = 145.7°$), Fig. 5 ($E_i = 106.0$ MeV, $\theta = 75°$), and Fig. 6 ($E_i = 81.0$ MeV, $\theta = 145.7°$). For an excitation energy of 25 MeV, the momentum transfer q for the three cases is 82, 115, and 131 MeV/c, respectively. The experimental points represent[27] the form factor

$$F_{\text{exp}}{}^2 = \frac{1}{\sigma_M} \frac{d^2\sigma}{d\Omega dE_f}\,, \tag{4}$$

where σ_M is the Mott cross section[27] and $d^2\sigma/d\Omega dE_f$ is the differential cross section at each final energy E_f.

For transitions from the ground state (g.s.) to a final state f, the theoretical form factors are given by[24,27]

$$F^2 = \frac{1}{\sigma_M}\left(\frac{d\sigma}{d\Omega}\right)^{\text{g.s.}\to f} = \frac{64\pi E_i{}^2 E_f{}^2 \sin^4\frac{1}{2}\theta}{Z^2 q^4}\left[\sum_{L=0}^{\infty}\frac{|\mathfrak{M}_L(q)|^2}{2J_i+1} + \frac{v_t(\theta)}{v_l(\theta)}\sum_{L=1}^{\infty}\frac{|\mathcal{T}_L^E(q)|^2 + |\mathcal{T}_L^M(q)|^2}{2J_i+1}\right], \tag{5a}$$

where

$$\frac{v_t(\theta)}{v_l(\theta)} = \frac{q^2}{(q^2-\omega^2)^2}\left[-2k_i k_f \sin^2\tfrac{1}{2}\theta + (k_i+k_f)^2\tan^2\tfrac{1}{2}\theta\right], \tag{5b}$$

ω is the excitation energy of the nucleus, k_i and k_f are the initial and final electron momenta, $\vec{q} = \vec{k}_i - \vec{k}_f$, and $\mathfrak{M}_L(q)$ and $\mathcal{T}_L^{E,M}(q)$ are the longitudinal and transverse matrix elements for electroexcitation, respectively.

It can be seen from Figs. 4–6 that our model predicts giant $E1$ and $M2$ transitions in remarkable

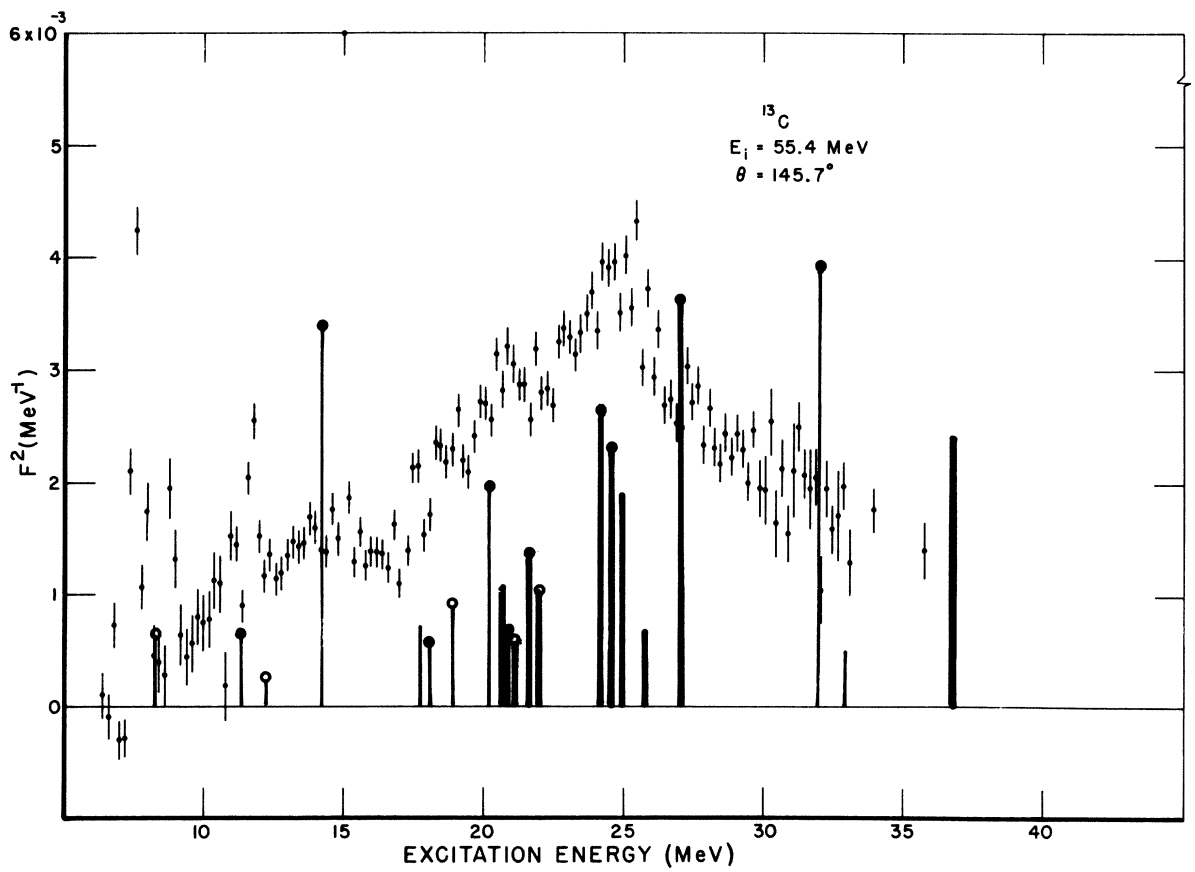

FIG. 4. Form factors for inelastic electron scattering from ^{13}C (see text for definitions). Incident electron energy $E_i = 55.4$ MeV, scattering angle $\theta = 145.7°$. The experimental points are from Bergstrom *et al.* (Ref. 27). Notation for the theoretical spikes is as follows: heavy lines: $T = \frac{3}{2}$, light lines: $T = \frac{1}{2}$, no top: $J = \frac{1}{2}$, open-circle top: $J = \frac{3}{2}$, and full-circle top: $J = \frac{5}{2}$. Average momentum transfer over the figure $q_{av} = 82$ MeV/c.

agreement with the experimental (e, e') data. This is especially true for the positions of the observed peaks, and to a good measure also for the momentum-transfer dependence of the form factors. The previously discussed isospin splitting of the giant resonance levels remain fairly pronounced, although the $T=\frac{3}{2}$ levels are shown to become dominant for the higher momentum transfers (see especially Fig. 6), and higher-spin states appear to play a very important role in the electroexcitation process.

The experimental peak at $E=15.11$ MeV is the well-known $M1$ level with spin and isospin J^π, $T=\frac{3}{2}^-, \frac{3}{2}$. Since our calculation includes only positive parity states, the theoretical spike close to the $E=15.11$ MeV peak should not be associated with the latter.

The squared matrix elements for the transverse $E1$ and $M2$ operators, i.e., $|\mathcal{T}_1^E|^2$ or $|\mathcal{T}_2^M|^2$, as well as for the longitudinal Coulomb operator $C1$, i.e., $|\mathfrak{M}_1|^2$, which are all dimensionless, are shown in Figs. 7–11. The initial state $J^\pi=\frac{1}{2}^-$ can couple through these operators only to final states with $J^\pi=\frac{1}{2}^+$, $\frac{3}{2}^+$ and $\frac{5}{2}^+$. Units are so chosen that the integral of the charge density over the nuclear volume is numerically equal to $Z=6$. Since Z also occurs in the denominator in Eq. (5a), the form factor is independent of the choice of this unit.

In these figures, one may recognize the states constituting the isospin mode and the spin-isospin modes of the giant dipole vibrations.[24] The isospin mode is characterized by transverse electric form factors having a maximum at $q=0$ and thus determining the shape of the photoabsorption cross sections; it is seen to consist of the $T=\frac{1}{2}$ states at $\omega=12.10$ and 17.92 MeV $(J=\frac{1}{2})$ as well as 20.25 and 20.87 MeV $(J=\frac{3}{2})$, clearly offset by isospin splitting from the $T=\frac{3}{2}$ states at $\omega=24.85$ and 25.76 MeV $(J=\frac{1}{2})$ as well as 24.35 and 24.57 MeV $(J=\frac{3}{2})$. The spin-isospin mode characteristically rises up with increasing momentum transfer and consists of $E1$ states $(J=\frac{1}{2}, \frac{3}{2})$ as well as $M2$ states $(J=\frac{3}{2}, \frac{5}{2})$ as shown in the figures.

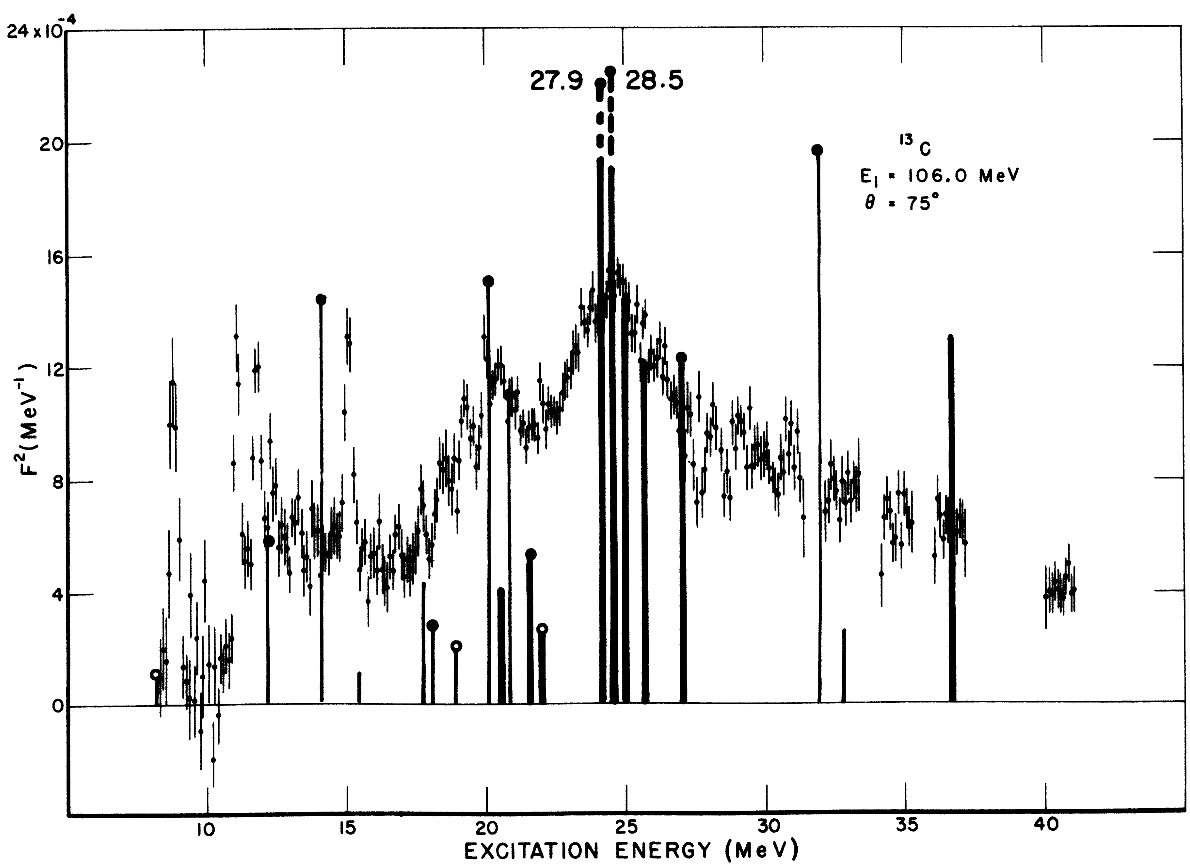

FIG. 5. Same as Fig. 4 except that $E_i=106.0$ MeV, $\theta=75°$, $q_{av}=115$ MeV/c. The height of two protruding states near 25 MeV is indicated by numbers.

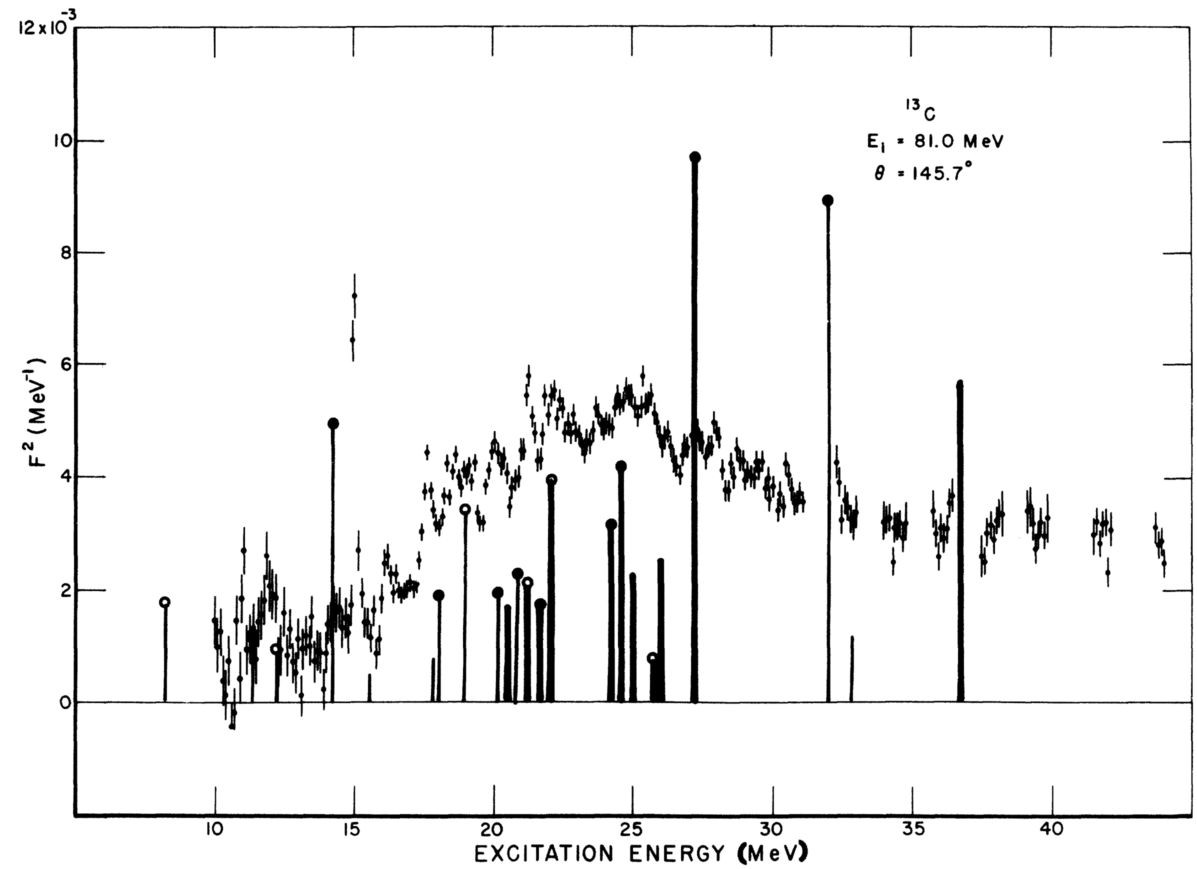

FIG. 6. Same as Fig. 4 except that $E_i = 81.0$ MeV, $\theta = 145.7°$, $q_{av} = 131$ MeV/c.

III. CALCULATION FOR ^{17}O

This calculation proceeded in a manner similar to that for ^{13}C; the main difference consists in the valence particle being in the s-d shell. This gives rise to a larger number of basis states; for example, there are 37 basis states for the $T = \frac{1}{2}$, $J = \frac{3}{2}$ case.

Promotion of valence particles up to the f-p shell is included in the calculation. The single-particle energies are given in Table I. Those for ^{17}O were taken from an article by Jolly.[42] The $1p_{1/2}$ and $1p_{3/2}$ hole energies are well established from the experimental spectra of ^{17}O and ^{15}O. The $1s$ hole (at 45 MeV) is uncertain in its energy by several MeV. The $1f_{7/2}$ level is found from an analysis of ^{16}O$(p,p)^{16}$O data,[43] where single-particle resonances are predicted by a smoothed set of optical parameters. The $1f_{7/2}$ resonance is at about 18 MeV. The $1f_{5/2}$, $2p_{3/2}$, and $2p_{1/2}$ levels have to be found in a different manner. The spin-orbit splitting for the $1f$ shell is taken to be ~7 MeV, putting the $1f_{5/2}$ level at 25 MeV. The $2p$ levels are chosen so that the order $1f_{7/2}$, $2p_{3/2}$, $1f_{5/2}$, $2p_{1/2}$ is preserved. The $2p_{3/2}$ level is taken arbitrarily at 23 MeV, and $2p_{1/2}$ at 26 MeV. Neutron energies are then found by reducing these values by the difference in binding energies of ^{17}F and ^{17}O. The harmonic oscillator parameter $b = 0.36$ fm^{-2} is taken from Carlson and Talmi,[44] this being a value typical of what is used also in other calculations for nuclei in the oxygen region.[34,45] The Soper interaction strength is taken as

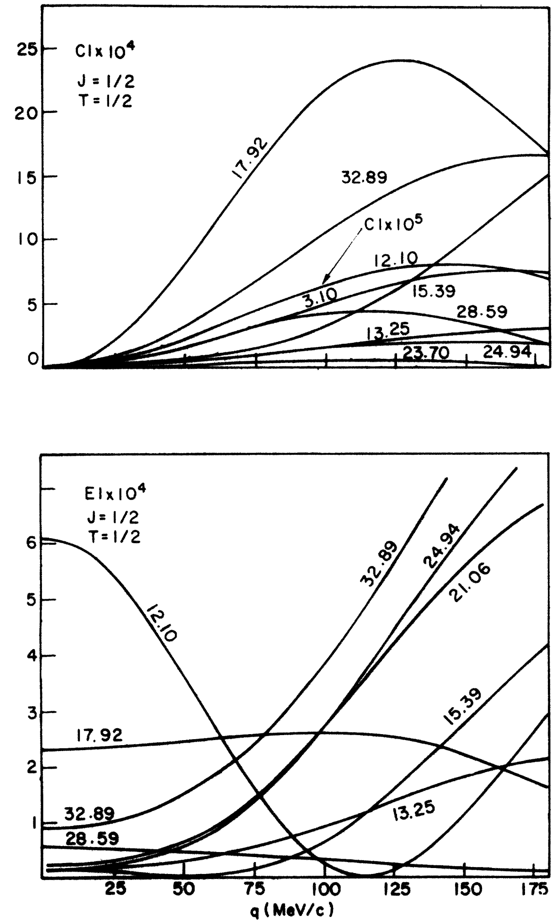

FIG. 7. Squared matrix elements of electric and magnetic operators as functions of the momentum transfer q for electron scattering from ^{13}C leaving the residual nucleus in excited state $J^\pi = \frac{1}{2}^+$, $T = \frac{1}{2}$. (See text for units.) The numbers refer to excitation energies (in MeV) of the states whose matrix elements are shown; matrix elements for additional states that were found smaller than those shown are disregarded.

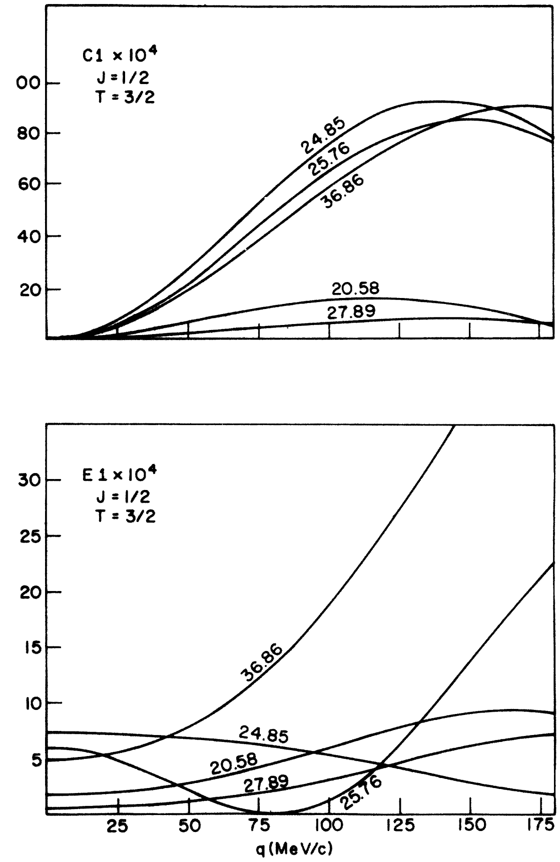

FIG. 8. Same as Fig. 7, for $J^\pi = \frac{1}{2}^+$, $T = \frac{3}{2}$ states.

$$V_0/4\pi b^3 = 8.25 \text{ MeV fm}^6 .$$

The theoretical electric dipole photoabsorption cross sections are shown in Figs. 12 and 13, as calculated with Soper (Fig. 12) and Tabakin (Fig. 13) interactions, and are compared in these figures with the measured $^{16}O(p, \gamma_0)^{17}F$ cross sections of Harakeh, Paul, and Gorodetzky.[12] Since the ground state (initial state) of ^{16}O can couple to the proton only to give a $T = \frac{1}{2}$ excited state in ^{17}F, the experimental points are to be compared with the theoretical $T = \frac{1}{2}$ (nonhatched) cross sections. The experiment gives only the differential cross section at $\theta = 90°$; so the comparison is only qualitative.

In both cases, the total ($T = \frac{1}{2}$ plus $\frac{3}{2}$) cross section shows a large maximum at 23 MeV. There is a minimum at ~26 MeV and a smaller maximum at 27 MeV in the Soper case and at 29 MeV in the Tabakin case. The figure indicates that in ^{17}O, one has a "giant resonance" peak at an energy below that of another "pygmy," resonance. The reason for this is that the giant peak is about half $T = \frac{1}{2}$ and half $T = \frac{3}{2}$. Accordingly, no clear cut isospin splitting of the giant resonance prevails in this nucleus. Some of the $T = \frac{3}{2}$ states have become somewhat depressed in energy, especially those carrying large dipole strengths; they are also characterized by large values of intermediate angular momentum coupling. For instance, large contributions to the giant peak come from $T = \frac{3}{2}$, $J = \frac{5}{2}$ states with intermediate angular momentum of 4.

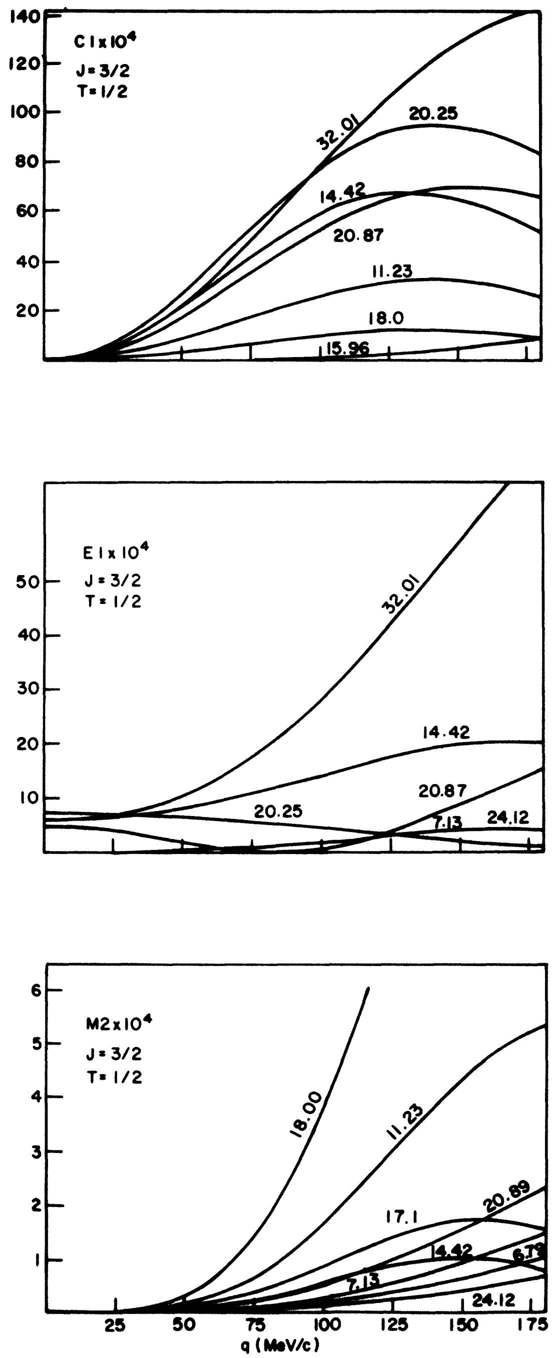

FIG. 9. Same as Fig. 7, for $J^{\pi}=\frac{3}{2}^{+}$, $T=\frac{1}{2}$ states.

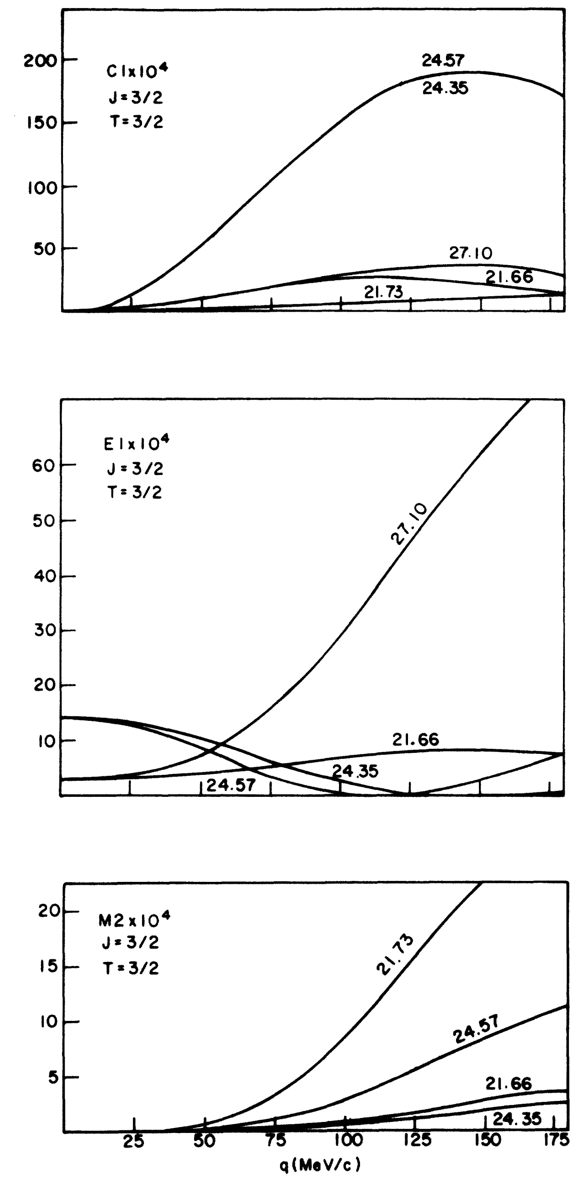

FIG. 10. Same as Fig. 7, for $J^{\pi}=\frac{3}{2}^{+}$, $T=\frac{3}{2}$ states.

These states are lowered in energy from the unperturbed value instead of being raised by the residual interaction. If this did not happen, the majority of strength would be in the peak at the higher energy. There is also a $T=\frac{3}{2}$ contribution to the spectrum at an energy $\gtrsim 35$ MeV in both cases.

No ^{17}O photonuclear experimental data are available in the giant resonance region which our calculated total cross sections could be compared to, the reason being the difficulty of obtaining a suitable target.

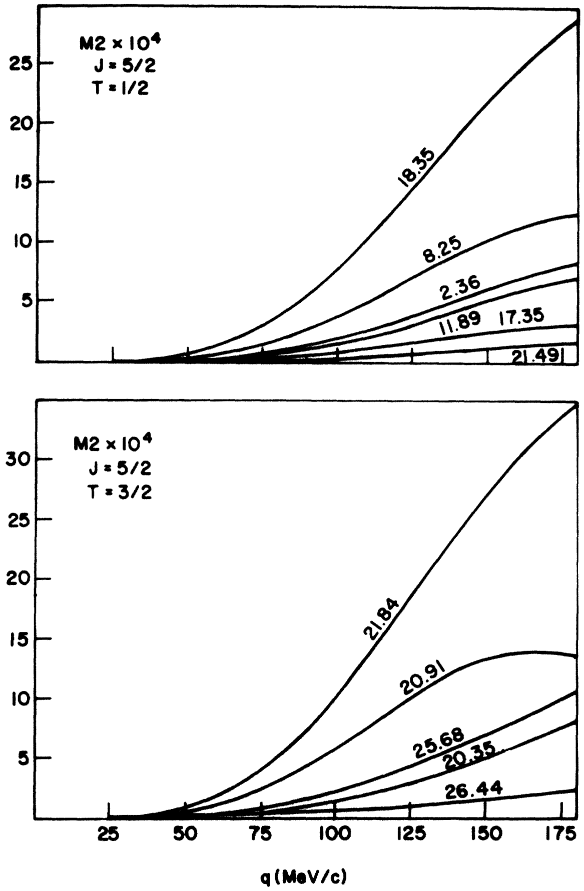

FIG. 11. Same as Fig. 7, for $J^\pi = \frac{5}{2}^+$, $T = \frac{1}{2}$ (top) and $T = \frac{3}{2}$ (bottom) states.

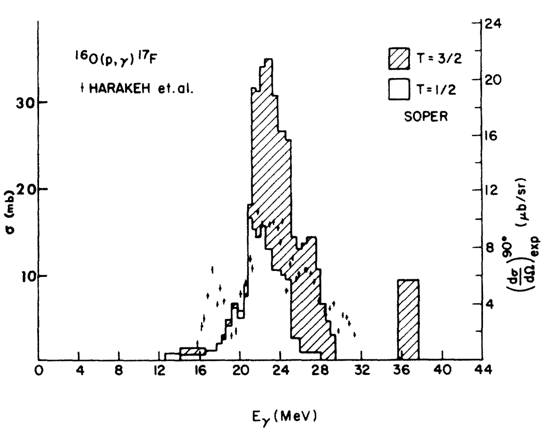

FIG. 12. Calculated electric dipole photoabsorption cross sections for ^{17}O using the Soper interaction, compared with ^{16}O$(p,\gamma_0)^{17}$F differential cross sections at $\theta = 90°$ measured by Harakeh *et al.* (Ref. 12).

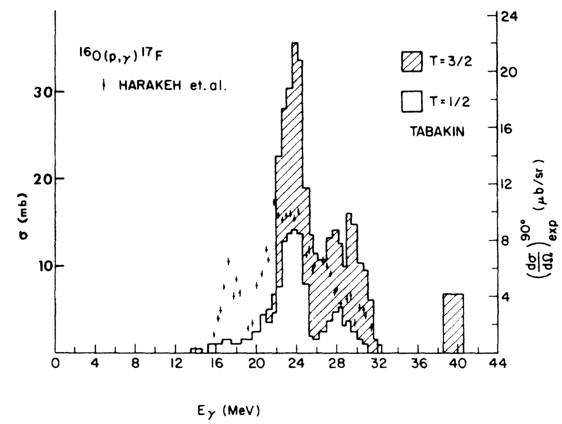

FIG. 13. Same as Fig. 7, using the Tabakin interaction.

IV. CONCLUSION

We have performed calculations using a two-particle, one-hole shell model for the giant resonances in ^{13}C and ^{17}O and have compared its predictions with measured photonuclear giant dipole resonances[3-6,12] and electron scattering form factors.[27] The model uses harmonic oscillator basis states and includes excitations of the valence particle, in addition to core excitations of the 1p-1h type. A modified zero range Soper interaction[14] and the separable Tabakin interaction[28] were employed for the residual forces. The modified Soper interaction reproduces both the giant and pygmy resonances in the ^{13}C photoabsorption cross sections, while the Tabakin interaction reproduces the qualitative features in the case of ^{17}O. (Quantitative comparison is not possible for ^{17}O, since only differential cross sections measured at $\theta = 90°$ are reported.)

The isospin sum rule given by O'Connell[30] was applied to the model, and its predictions using both the modified Soper and Tabakin interactions were compared with the experimental and the expected theoretical values. The Soper potential produces significantly better agreement than the Tabakin potential. Electron scattering form factors for ^{13}C, which were also calculated with the former potential, show good agreement with the experimental results of Bergstrom *et al.*[27]

We wish to thank Professor Hall L. Crannell and Dr. A. M. Saruis for useful discussions, and Mr. B. A. Lamers for some helpful contributions.

*Present address: Systems, Science and Software, La Jolla, California 92037.
†Present address: Bureau of Radiological Health, Rockville, Maryland 20852.
‡Supported in part by a grant of the National Science Foundation.
[1]M. Danos and E. G. Fuller, Annu. Rev. Nucl. Sci. 15, 29 (1965).
[2]B. M. Spicer, in *Advances in Nuclear Physics*, edited by M. Baranger and E. Vogt (Plenum, New York, 1969), Vol. 2, Chap. 1.
[3]Barnett C. Cook, Phys. Rev. 106, 300 (1957).
[4]E. G. Muirhead, B. M. Spicer, and M. N. Thompson, Atomic and Nuclear Interactions of High Energy Photons and Electrons with Matter, Technical Report, School of Physics, University of Melbourne, 1975 (unpublished).
[5]B. L. Berman, Atlas of Photoneutron Cross Sections Obtained with Monoenergetic Photons, Technical Report, Lawrence Livermore Laboratory, Livermore, California, 1976 (unpublished).
[6]V. P. Denisov, A. V. Kulikov, and L. A. Kulchitskii, Zh. Eksp. Teor. Fiz. 46, 1488 (1964) [Sov. Phys. JETP 19, 1007 (1964)].
[7]R. E. Marrs *et al.*, Phys. Rev. Lett. 35, 202 (1975).
[8]K. Fukuda, Nucl. Phys. A156, 10 (1970).
[9]P. S. Fisher *et al.*, Nucl. Phys. 45, 113 (1963).
[10]C. Rolfs and R. E. Azuma, Nucl. Phys. A227, 291 (1974).
[11]M. Hasinoff, D. Johnson, and D. F. Measday, Phys. Lett. 39B, 506 (1972).
[12]M. N. Harakeh, P. Paul, and Ph. Gorodetzky, Phys. Rev. C 11, 1008 (1975).
[13]S. Fallieros, B. Goulard, and R. H. Ventner, Phys. Lett. 19, 398 (1965); S. Fallieros, T. A. Hughes, and B. Goulard, Proceedings of the Williamsburg Conference on Intermediate Energy Physics, College of William and Mary, Williamsburg, 1966 (unpublished), p. 743; B. Goulard and S. Fallieros, Can. J. Phys. 45, 3221 (1967).
[14]B. R. Easlea, Phys. Lett. 1, 163 (1962).
[15]M. Gell-Mann and V. L. Telegdi, Phys. Rev. 91, 169 (1953).
[16]P. Axel *et al.*, Phys. Rev. Lett. 19, 1343 (1967).
[17]E. Hayward, *Nuclear Structure and Electromagnetic Interactions* (Plenum, New York, 1965), p. 141.
[18]The $T_< \equiv \frac{1}{2}$ vs $T_> \equiv \frac{3}{2}$ character of a given state can here be assigned by a comparison of the resonances appearing in $^{13}C(\gamma, n$ or $p)$ with those appearing in the inverse reaction $^{12}C(p, \gamma_0)$, since in the former case both $T=\frac{1}{2}$ and $\frac{3}{2}$ states are formed, in the latter case only $T=\frac{1}{2}$ states.
[19]O. Titze, A. Goldman, and E. Spamer, Phys. Lett. 31B, 565 (1970).
[20]D. J. Albert, Ph.D. thesis, The Catholic University of America, June 1969 (unpublished).
[21]G. E. Brown, *Unified Theory of Nuclear Models and Forces* (Wiley, New York, 1967).
[22]D. J. Albert, R. F. Wagner, H. Überall, and C. Werntz, Bull. Am. Phys. Soc. Ser. II 14, 606 (1969). For the analogous case of ^{5}He, the results of this model have been applied to the reaction $t+d \rightarrow {}^4$He $+n+\gamma$: R. F. Wagner, C. Werntz, D. J. Albert, and H. Überall, Bull. Am. Phys. Soc. Ser. II 14, 535 (1969); R. F. Wagner and C. Werntz, Phys. Rev. C 4, 1 (1971).
[23]A similar calculation of these giant resonance states using a continuum shell model has recently been brought to our attention: M. Marangoni, P. L. Ottaviani, and A. M. Saruis, Nucl. Phys. A277, 239 (1977).
[24]See, e.g., H. Überall, *Electron Scattering from Complex Nuclei* (Academic, New York, 1971).
[25]H. Überall, Nuovo Cimento 41, 25 (1966).
[26]H. Überall, Springer Tracts Mod. Phys. 49, 1 (1969).
[27]J. C. Bergstrom, Hall Crannell, F. J. Kline, and J. T. O'Brien, Phys. Rev. C 4, 1514 (1971).
[28]F. Tabakin, Ann. Phys. (N.Y.) 30, 51 (1964).
[29]E. Baranger and C. W. Lee, Nucl. Phys. 22, 157 (1961).
[30]James O'Connell, Phys. Rev. Lett. 22, 1314 (1969).
[31]N. Vinh-Mau and G. E. Brown, Nucl. Phys. 29, 89 (1962).
[32]H. Tyren, P. Hillman, and Th. A. J. Maris, Nucl. Phys. 7, 10 (1958); T. J. Gooding and H. G. Pugh, *ibid.* 18, 46 (1960).
[33]J. R. McGruer, E. K. Warburton, and L. S. Bender, Phys. Rev. 100, 235 (1955).
[34]F. H. Lewis and J. D. Walecka, Phys. Rev. 133, B849 (1964).
[35]D. Clement and E. Baranger, Nucl. Phys. A108, 27 (1968).
[36]In the case of Tabakin potential, second-order corrections to the residual interaction (restricted to $2\hbar\omega$ excitations) were taken into account following the procedure of B. R. Barrett, Phys. Rev. 154, 955 (1967).
[37]The dipole strengths generated by the isoscalar ($\Delta T = 0$) part of the dipole operator were found to be small at the photon point, exciting mainly spurious states which have been removed from the wave function. As q increases (in electron scattering), the isoscalar part excites more than just the spurious state and can contribute significantly to the strength of the matrix element.
[38]This separation is also evident in the electron scattering data (Ref. 27), see below.
[39]A Tabakin calculation including the added strength of Eq. (2) resulted in considerably less splitting of the giant resonance. This shows that the detailed nature of the residual interaction determines the resonance structure.
[40]H. R. Collard, L. R. B. Elton, and R. Hofstadter, *Nuclear Radii* (Springer, Berlin, 1967).
[41]Evans Hayward, *Photonuclear Reactions*, NBS Monograph No. 118, U.S. Department of Commerce, 1970.
[42]P. Jolly, Phys. Lett. 5, 289 (1963).
[43]G. Hardie, R. L. Dangle, and L. D. Oppliger, Phys. Rev. 129, 353 (1963).
[44]B. C. Carlson and I. Talmi, Phys. Rev. 96, 436 (1957).
[45]C. Quesne, Nucl. Phys. 76, 268 (1965).